# Asialoglycoprotein Receptor (ASGP-R) in Liver Parenchymal Cells is Involved in Elimination of Recombinant Human TFPI

Running head: Recombinant Human $TFPI^{BHK}$ is cleared via the liver ASGP-R

Cristina Ionica Øie[1], Ellen Brodin[1], Rupa Shree Appa[2], Bård Smedsrød[3], John-Bjarne Hansen[1].

[1]Center for Atherothrombotic Research (CART), Department of Medicine, Institute of Clinical Medicine, University of Tromsø, Tromsø, Norway, [2]Biopharmaceuticals Research Unit, Novo Nordisk, Måløv, Denmark, and [3]Vascular Biology Research Group, Institute of Medical Biology, University of Tromsø, Tromsø, Norway.

Correspondence to: Cristina Ionica Øie, Center for Atherothrombotic Research in Tromsø (CART), Department of Medicine, Institute of Clinical Medicine, University of Tromsø, NO-9037 Tromsø, Norway. Telephone: + 47 776 44686; Fax: +47 77645400, cristina.ionica.oie@uit.no

## ABSTRACT

We here report on a study carried out to determine the early clearance kinetics, and organ, cell(s) and receptor(s) responsible for the clearance of full length TFPI purified from BHK cells ($TFPI^{BHK}$). Following intravenous administration, $^{125}I\text{-}TFPI^{BHK}$ was cleared with a biphasic elimination curve, and with a significantly slower $t_{1/2}\alpha$ compared to recombinant human TFPI from *E.Coli* ($TFPI^{E.Coli}$) (1.95±0.10 versus 1.42±0.07 min, respectively, $p<0.001$). Studies on organ and cell distribution revealed that liver parenchymal cells (PCs) were responsible for 96% of the uptake of $TFPI^{BHK}$ and 81% of $TFPI^{E.Coli}$, whereas the non-parenchymal cells (NPCs) were responsible for 4% and 19%, respectively. Pre-administration of excessive amounts of unlabeled $TFPI^{BHK}$ prolonged blood clearance of $^{125}I\text{-}TFPI^{BHK}$. Unlabelled $TFPI^{BHK}$ inhibited endocytosis of $^{125}I\text{-}TFPI^{BHK}$ in PCs *in vitro*, whereas blocking of LDL-receptor related protein-1 (LRP-1) by receptor-associated protein (RAP) affected neither blood clearance nor endocytosis of $^{125}I\text{-}TFPI^{BHK}$ in PCs. In addition, $TFPI^{BHK}$ was also found in the kidneys and this could be reduced in the presence of RAP. Asialoorosomucoid (ASOR), a potent inhibitor of the asialoglycoprotein receptor (ASGP-R), prolonged the circulatory survival of $^{125}I$-m-TFPI by 1.5-fold ($p<0.001$). *In vitro*, ASOR and other ASGP-R antagonists significantly inhibited endocytosis of $^{125}I\text{- }TFPI^{BHK}$ in PCs. Moreover, unlabelled $TFPI^{BHK}$ markedly decreased endocytosis of $^{125}I$-asialofetuin. In conclusion, our findings suggest that ASGP-R mediated endocytosis in the liver is involved in the clearance of $TFPI^{BHK}$.

## INTRODUCTION

Tissue factor pathway inhibitor (TFPI) is an endogenous serine protease inhibitor of tissue factor (TF)-induced blood coagulation [1] which exerts its function by neutralizing the catalytic activity of factor Xa (FXa), and by feedback inhibition of the factor VIIa-TF complex in the presence of FXa [2, 3]. The translated amino acid sequence from the human TFPI cDNA clone consists of 276 amino acids with 18 cysteines, and two potential N-linked glycosylation sites and one O-glycosylation site, with a predicted MW of 32 kDa [4] and an actual MW estimated from SDS PAGE of about 42 kDa due to glycosylations [5].

The use of selective pharmacological inhibitors has become an indispensable tool in experimental haemostasis and thrombosis research, in which recombinant TFPI (rTFPI) may be a beneficial therapeutic agent as a natural anticoagulant to attenuate pathological clotting activation [6, 7]. Half-life extension is desirable when designing recombinant therapeutic proteins. So far, two major types of rTFPI were purified and used in animal studies and human clinical trials. The non-glycosylated form of rTFPI, produced by *E.Coli* ($TFPI^{E.Coli}$), has been shown to be rapidly cleared from the circulation with a plasma half-life of less than 1 minute in rats [8]. In vivo and in vitro studies implicate LRP-1 in degradation and clearance of $TFPI^{E.Coli}$ [9, 10] and haparan sulfate proteoglycans (HSPGs) have been identified as the receptors in a second receptor system that is involved in the in vivo clearance of $TFPI^{E.Coli}$ [9, 11].

Mammalian cells have become the dominant system for the production of recombinant proteins for clinical applications because of their capacity for proper protein folding, assembly and post-translational modifications. Thus, the quality and efficacy of a protein can be superior when expressed in mammalian cells versus other hosts such as bacteria, plants and

yeast [12]. Recombinant glycosylated TFPI has been purified from several mammalian cell lines. rTFPI expressed in mouse C127 ($TFPI^{C127}$) fibroblasts has been shown to have a different route of elimination compared to $TFPI^{E.Coli}$ [13]. This type of TFPI had substantially prolonged survival in the circulation and simultaneous administration of RAP did not affect the survival of $TFPI^{C127}$ in the circulation. Furthermore, excessive amounts of unlabeled $TFPI^{C127}$ did not affect binding and degradation of $^{125}$I-labeled $TFPI^{E.Coli}$ in HepG2 cells [13]. Anatomical distribution studies showed that while $TFPI^{E.Coli}$ is mainly found in the liver of rats [8], $TFPI^{C127}$ and rTFPI expressed in human SK hepatoma cells ($TFPI^{SK}$) are found both in liver and in kidneys of rabbits [14].

Human recombinant full length TFPI expressed in baby hamster kidney cells (BHK) ($TFPI^{BHK}$) was used in this study. This type of TFPI was first purified in 1990 [15]. The molecular properties were comparable with that observed for rTFPI synthesized by HepG2 and HeLa cells, and the authors suggested that this type of TFPI could be used as adjunct therapy in the treatment of some thrombotic diseases. Pharmacokinetics studies in rabbits showed that $TFPI^{BHK}$ is cleared with a $t_{1/2}\beta$ of 16.8 min [16]. In the present study we aimed to carry out a more detailed PK study during the first phase of clearance, to identify the organ(s) involved in removal of $TFPI^{BHK}$ from the circulation and to determine the hepatocellular site of uptake, as well as to identify the main cell (s) and their receptor(s) involved in the clearance.

## MATERIALS AND METHODS

### Animals

Male albino rats, Sprague-Dawley (mean body weight 200-250 g), purchased from Scanbur BK, AB (Sollentuna, Sweden) were kept under controlled animal conditions, and fed a standard chow (Scanbur BK, Nittedal, Norway) *ad libitum*. For *in vivo* experiments, anesthesia was induced with 4% Isofluran (Abbott Scandinavia AB, Solna, Sweden) and maintained at 2.1%. For *in vitro* studies, rats were anesthetized by subcutaneous injection of a mixture of 0.4 mg/kg Domitor (Orion Pharma, Espoo, Finland) and 60 mg/kg Ketalar (Pfizer AS, Lysaker, Norway). All experimental protocols were approved by the Norwegian Animal Research Authority in accordance with the Norwegian Animal Experimental and Scientific Purposes Act of 1986.

### Materials:

Human recombinant full length TFPI, 42 kDa, isolated from Baby Hamster Kidney cell line (BHK) ($TFPI^{BHK}$) [15] was from Novo Nordisk (Måløv, Denmark). Human recombinant full length TFPI, 35 kDa, isolated from *E.Coli* ($TFPI^{E.Coli}$) was obtained from American Diagnostica Inc (Greenwich, CT, USA). Receptor associated protein (RAP) purified from *E.Coli* strain BL21(DE3) (Invitrogen, Taastrup, Denmark) was from Novo Nordisk (Måløv, Denmark). Carrier free $Na^{125}I$ was from Perkin-Elmer Norge AS (Oslo, Norway), and 1,3,4,6-tetrachloro-3α, 6α-diphenylglycoluril (Iodogen) was from Pierce Chemical Co. (Rockford, IL, USA). Collagenase P was from Worthington Biochemical Corporation (Lakewood, NJ, USA). Human serum albumin (HSA) was from Octapharma (Ziegelbrucke, Switzerland). Culture media D-MEM/F-12 and RPMI 1640 supplemented with 50 U/ml penicillin and 50 μg/ml streptomycin were from Gibco BRL (Roskilde, Denmark). Fluorescein isothiocyanate (FITC), Protamine, Glycine, Asialofetuin, type II from fetal calf serum, Galactose and Ovalbumin

were from Sigma Co (St. Louis, MO, USA). Phosphotungstic acid (PTA) was from Merck (Darmstadt, Germany). Bovine serum albumin, fraction 5 (BSA) was from ICN Bichemicals Inc., (CA, USA). Sephadex G-25 columns (PD-10) and Percoll were from Amersham Biotech (Uppsala, Sweden). Asialoorosomucoid (ASOR) was prepared via enzymatic hydrolysis of orosomucoid (Sigma Aldrich Inc., St. Louis, MO, USA) following the manufacturer's instructions. ASOR was characterized by isoelectric focusing analysis using Novex® IEF gels from Invitrogen Life Technologies (Carlsbad, CA, USA) [17]. Asialo-FVIIa was prepared by desialylation of FVIIa (Novo Nordisk, Måløv, Denmark) using neuraminidase according to the manufacturer's protocol (New England Biolabs, Inc., UK). Formaldehyde treated serum albumin (FSA) was prepared as described [18].

**Radiolabeling**

Macromolecular ligands ($TFPI^{E.Coli}$ and $TFPI^{BHK}$) in PBS were labelled with carrier-free $Na^{125}I$ in a direct reaction employing iodogen as oxidizing agent [19]. The ligands and activated $^{125}I$ were allowed to react for 30 min and the reaction was stopped by the addition of $Na_2S_2O_5$ and excess amount of KI. Radiolabeled ligands and free iodine were separated by gel filtration on a PD-10 column equilibrated with 1% HSA in PBS. Fractions of 0.5 ml were collected with PBS as eluting buffer. Radioactivity was measured using a gamma-counter (Cobra II, Packard, New York, NT, USA). The resulting specific radioactivities were between 3.2 – 4.4 x $10^7$cpm/μg. To prevent escape of marker isotope from the site of uptake, $TFPI^{BHK}$ was labelled with FITC [20]. Unbound FITC was removed by gel filtration on a PD-10 column.

**Blood Clearance and Anatomical Distribution**

Blood clearance and anatomical distribution of i.v. administered $^{125}I$-TFPI was determined as described [21]. Briefly, $^{125}I$- $TFPI^{E.Coli}$ and $^{125}I$- $TFPI^{BHK}$ (0.60 μg/kg in 0.25 ml physiological

saline) were injected in the tail vein. Specificity of blood clearance of $TFPI^{BHK}$ was investigated by injecting $^{125}I$- $TFPI^{BHK}$ alone (0.60 μg/kg; 0.5 nM) or 1 min after injection of RAP (50 mg/kg); or 200 fold molar excess of unlabelled $TFPI^{BHK}$, or Protamine (40 mg/kg) and 200 fold molar excess of unlabelled $TFPI^{BHK}$, or ASOR (15mg/kg). Blood samples (25 μl) were collected from the tip of the tail and mixed with 0.5 ml water and 0.75 ml of 20% TCA, 0.5% PTA to precipitate undegraded protein and high molecular weight peptides. Radioactivity in the supernatant after centrifugation (acid-soluble radioactivity) was taken as degraded TFPI. Radioactivity in blood 0.5 min after injection was defined as 100%, and the percentage of radioactivity remaining in the circulation was calculated.

Anatomical distribution was assessed 10 min, 20 min, 1h, 2h and 4h after i.v. administration of $^{125}I$- $TFPI^{E.Coli}$ or $^{125}I$- $TFPI^{BHK}$. The abdomen was cut open and the organs were washed free of blood by systemic perfusion through the heart with physiological saline. The following organs were analyzed for radioactivity: liver, spleen, kidneys, stomach, intestines, urine, lungs, heart, eyes, brain, tail, muscle, thymus, testicles and blood. Total blood volume of each rat was calculated according to Waynforth and Flecknell [22].

**Fluorescence Microscopy**

At 15 min following i.v. administration of 30 μg/kg FITC- $TFPI^{BHK}$ in 0.5 ml physiological saline, liver and kidneys were dissected out, fixed in 4% formaldehyde, prepared and sectioned for fluorescence microscopy. Sections were examined with an Axiophot photomicroscope (Carl Zeiss, Oberkochen, Germany). Photomicrographs were taken with a Nikon DS 5MC digital camera.

**Hepatocellular Distribution**

The distribution of radiolabelled ligands in different liver cell populations was assessed 15 min following i.v administration of $^{125}$I- TFPI$^{E.Coli}$ and $^{125}$I- TFPI$^{BHK}$ (2.5 μg/kg) by quantifying the amount of radioactivity per million cells of parenchymal cells (PCs) and non-parenchymal cells (NPCs). NPC fraction consists mainly of liver sinusoidal endothelial cells (LSECs) and Kupffer cells (KCs) and is essentially devoid of PCs, red blood cells, stellate cells and debris. Cell numbers were assessed by visual counting in a phase contrast microscope. The uptake per cell was calculated based on the fact that the ratio between KCs, LSECs and PCs in rat liver is 1:2.5:7.7 [23]. The method for determining the hepatocellular distribution of different ligands has previously been used by us and others [21, 24, 25].

**Isolation and Cultivation of Liver Cells**

The method for preparation of pure cultures of functionally intact PCs, LSECs and KCs from a single rat liver has been described elsewhere [26]. Briefly, the liver was perfused with collagenase, and the resulting single cell suspension was subjected to velocity and density centrifugations to produce PCs and NPCs. The PCs were centrifuged at 50 x g and the resulted pellet washed 5 times with D-MEM/F-12. The cells were resuspended in D-MEM/F-12 containing 1% HSA. 0.4 x $10^6$ PCs were seeded on 2 $cm^2$ diameter culture dishes from Becton Dickinson Labware (Le Pont de Claix, France) coated with 0.1% collagen in PBS and incubated in humidified air with 5% $CO_2$ at 37°C for 4 to 6 h to allow cell attachment.

**Endocytosis Studies**

Unattached PCs were removed by washing with PBS immediately prior to each endocytosis experiment. Fresh D-MEM/F-12 with 1% HSA and 0.5 nM $^{125}$I- TFPI$^{BHK}$ alone or together with excess amounts of unlabelled potentially inhibitory agents such as TFPI$^{BHK}$ (500-fold), RAP, ASOR, asialofetuin, asialo-FVIIa, ovalbumin (100 μg/ml) or galactose (50 mM). To

assess the impact of heparan sulfate proteoglycans (HSPGs) on $^{125}$I- TFPI$^{BHK}$ binding and degradation, the cells were preincubated for 5 min with protamine (100 μg/ml) [9], before addition of the $^{125}$I- TFPI$^{BHK}$. Binding studies were carried out for 2 h at 4°C to avoid internalization of the ligand. Endocytosis studies were carried out for 2 h at 37°C. Endocytosis studies were terminated by transferring the cell media (200 μl) along with one wash of PBS (500 μl) to empty tubes and mixed with cold 20% TCA, 0.5% PTA (750 μl). Ligand degradation was determined by measuring the amount of labeled acid soluble radioactivity after centrifugation. Cell-associated ligand was quantified by measuring the radioactivity in the washed cells solubilized in 1% SDS. The functionality of the PCs and their endocytic receptors LRP-1 and ASGP-R were tested with $^{125}$I-RAP and $^{125}$I-ASOR or $^{125}$I-asialofetuin, respectively.

Opossum kidney cells (OK) (passages 39-44), which are considered representative of renal proximal tubules [27, 28] were routinely cultured in plastic flasks (25 cm$^2$) using culturing medium DMEM/F-12 supplemented with 10 % FBS, 50 U/ml penicillin and 50 μg/ml streptomycin. At confluence the cells were washed twice in PBS and detached by adding 1 ml 0.5 % trypsin/EDTA for 10min. The cells were thereafter seeded (25.000 cells/cm$^2$) in 24-well plates (Costar, Acton, MA, USA). Fresh medium was added every 48 h. Endocytosis was performed by incubating the OK cells for 1h at 37°C with D-MEM/F-12 medium, 1% HSA containing 1 nM $^{125}$I- TFPI$^{BHK}$ alone or in the presence of 500 nM RAP. The amount of $^{125}$I-TFPI$^{BHK}$ bound to the cells was measured after washing the cells with a solution of 0.1 Glycine, pH 2.4. Internalized $^{125}$I- TFPI$^{BHK}$ was quantified by measuring the amount of label released by treating washed cultures with a solution of 1% SDS.

**Statistics**

All data are presented as the means ± SEM unless otherwise indicated. We analyzed numeric data for statistical significance using Student's unpaired t-test with Prism software (GraphPad). *P* values of less than 0.05 were considered statistically significant. Clearance kinetics were analyzed as described previously [20].

## RESULTS

*Blood clearance*

Elimination of $^{125}$I- TFPI$^{BHK}$ and $^{125}$I- TFPI$^{E.Coli}$ were determined by measuring the decay of radioactivity in blood samples collected over time after i.v. injection of trace amounts (0.25 μg/kg) of radiolabeled ligands into the tail vein of rats. The kinetics of elimination followed a biphasic pattern for both types of TFPI (Figure 1). The clearance during the initial and rapid $\alpha$-phase ($t_{1/2}\,\alpha$) was significantly slower for TFPI$^{BHK}$ than for TFPI$^{E.Coli}$ (1.95 ± 0.10 and 1.42 ± 0.07 min, respectively ($p$<0.001, n=10 in each group)), but not significantly different during the terminal slow $\beta$-phase ($t_{1/2}\,\beta$) (25.47 ± 1.47 and 29.90 ± 3.22 min, respectively ($p$=0.20)). Measurements of acid soluble radioactivity in the blood samples, representing degradation of labeled ligand, revealed that 6.2 ± 1.3% of TFPI$^{BHK}$ and 3.8 ± 1.9% of TFPI$^{E.Coli}$ ($p$=0.01) were degraded about 20 min after administration. In contrast to what was found for TFPI$^{E.Coli}$, a modest increase in degraded material of TFPI$^{BHK}$ continues during the observation time.

*Anatomical distribution*

Organ distribution examined 10 min after injection revealed that the liver is the main organ for uptake of TFPI$^{E.Coli}$, with 40% of the recovered radioactivity (Figure 2A), while TFPI$^{BHK}$ was found in similar amounts in liver and kidneys, with about 25% of the recovered radioactivity in each of the two organs (Figure 2B). The radioactivity in the primary organs of uptake declined over time with a concomitant accumulation in the gastrointestinal tract. Only trace amounts of radioactivity accumulated in the urine and other organs at any time point. The radioactivity recovered in the circulation decreased gradually over time from 32 ± 1% at 10 min to 7 ± 1% at 4 h after $^{125}$I- TFPI$^{E.Coli}$ administration ($p$ for trend <0.001), and from 41 ± 5% at 10 min to 16 ± 4% at 4 h after $^{125}$I- TFPI$^{BHK}$ administration ($p$ for trend <0.001).

*Fluorescence microscopy*

Fluorescence microscopy of random liver and kidney sections fixed 15 min after administration of FITC- $TFPI^{BHK}$ revealed accumulation of fluorescence in both organs (Figure 3), similar to observations from the anatomical distribution study. In the liver, fluorescence was observed both in the parenchymal cells (mainly in the pericentral areas) (Figure 3A) and in the non-parenchymal cells represented by the cells lining the liver sinusoids (in periportal areas) (Figure 3B). In kidneys, the fluorescence was observed in the outer cortex, mainly in cells of the proximal convoluted tubules (Figure 3C) and minor amounts in glomeruli (Figure 3D).

*Hepatocellular distribution*

The observation that TFPI was taken up by the liver prompted us to investigate the distribution of radiolabelled ligands in the different cell populations. The liver cells were isolated 15 min after injection of $^{125}$I- $TFPI^{BHK}$ and $^{125}$I- $TFPI^{E.Coli}$, and the radioactivity was measured in parenchymal cells and non-parenchymal cells. The distribution revealed that PCs were responsible for the main uptake of both types of TFPI (Table 1). Based on the relative distribution of the cells in intact liver, it could be calculated that the total cell population of PCs were responsible for 96% ± 2% of the uptake of $TFPI^{BHK}$ and 81% ± 12% of $TFPI^{E.Coli}$, whereas the NPCs were responsible for 4% ± 2% and 19% ± 12%, respectively.

*Specificity of blood clearance*

In order to determine the specificity of the clearance of $^{125}$I- $TFPI^{BHK}$ *in vivo*, rats were injected i.v. with $^{125}$I- $TFPI^{BHK}$ (0.60 μg/kg) with or without pre-administration of a 200-fold molar excess of unlabeled $TFPI^{BHK}$, recombinant RAP (50 mg/kg) as competitor for the LRP-1, ASOR (15 mg/kg) as competitor for the asialo glycoprotein receptor, or 40 mg/kg protamine [9] as competitor for HSPGs sites involved in binding of $TFPI^{BHK}$ (Table 2). Pre-

administration of unlabelled $TFPI^{BHK}$ caused a marked prolongation of the $\alpha$- and $\beta$-phase, whereas administration of RAP prior to $^{125}$I- $TFPI^{BHK}$ did not affect the plasma clearance of $TFPI^{BHK}$. ASOR, a ligand with high affinity for the ASGP-R [29, 30], significantly prolonged the rapid $\alpha$-phase by 1.5-fold ($p$=0.001) and had no effect on the slow $\beta$-phase of $TFPI^{BHK}$ clearance (Table 2). Pre-injection with protamine had no significant impact on the clearance of $^{125}$I-$TFPI^{BHK}$.

*Endocytosis in primary cultures of PCs*

Endocytosis of both forms of TFPI was monitored in primary cultures of PCs isolated from rat liver. The cells were incubated with 0.5 nM $^{125}$I- $TFPI^{E.Coli}$ (Figure 4A) or $^{125}$I- $TFPI^{BHK}$ (Figure 4B), and radioactivity associated with the cells or with degradation products in the medium were measured at various time periods. The endocytosis increased almost linearly over time for both ligands and accounted for 65 ± 13 fmol/$10^6$ PCs of added $^{125}$I- $TFPI^{E.Coli}$ and 44 ± 4 fmol/$10^6$ PCs of added $^{125}$I- $TFPI^{BHK}$ after 4 h of incubation. Degradation products were detected after 30 min of incubation, and 31 ± 10 fmol/$10^6$ PCs and 23 ± 2 fmol/$10^6$ PCs of $^{125}$I- $TFPI^{E.Coli}$ and $^{25}$I- $TFPI^{BHK}$, respectively, were degraded after 4 h of incubation.

To determine the role of HSPGs in cellular binding and degradation of $^{125}$I- $TFPI^{BHK}$ in primary cultures of PCs, the cells were pretreated with 100μg/ml protamine, a concentration previously shown to inhibit 90% of $^{125}$I- $TFPI^{E.Coli}$ binding to $MH_1C_1$ cells [9]. Protamine only caused a modest, but not significant increase in cellular binding of $TFPI^{BHK}$ (11 ± 5%) without affecting cellular degradation (Figure 5).

To investigate the specificity of $TFPI^{BHK}$ endocytosis in PCs, 500-fold molar excess of unlabelled $TFPI^{BHK}$ was added together with 0.5 nM $^{125}$I- $TFPI^{BHK}$ and incubated for 2 h at 4°C to assess cellular binding, or at 37°C to assess endocytosis. Excessive amounts of

unlabeled $TFPI^{BHK}$ inhibited total endocytosis by 81 ± 1% ($p$<0.001), and cellular degradation by 91 ± 3% ($p$<0.001) (Figure 5), suggesting that the uptake of $TFPI^{BHK}$ in PCs is receptor mediated. Furthermore, cross-competitive binding studies with radiolabeled $TFPI^{BHK}$ and $TFPI^{E.Coli}$ (0.5 nM) and excess amounts of unlabeled $TFPI^{E.Coli}$ and $TFPI^{BHK}$ (100- and 500-fold molar), respectively caused no reciprocal inhibition of cellular binding and endocytosis (data not shown). Excess amounts of RAP had no significant affect on cell-association or degradation of $TFPI^{BHK}$ (Figure 5).

The prolonged circulatory survival of $TFPI^{BHK}$ observed after pre-administration of ASOR, encouraged us to further investigate cellular binding and endocytosis of $TFPI^{BHK}$ by ASPGP-R in primary cultures of PCs *in vitro*. Thus, we incubated PCs with trace amounts of $^{125}$I-$TFPI^{BHK}$ in the presence or absence of high concentration of unlabelled ligands known to bind to the ASGP-R (Figure 6A). ASOR, asialofetuin and asialo-FVIIa had a marked impact on $TFPI^{BHK}$ endocytosis, inhibiting both the cell-association and degradation by more than 87% ($p$<0.001). Galactose and ovalbumin inhibited also significantly the endocytosis of $TFPI^{BHK}$, but to a lesser extent than the previous three ligands; by 63 ± 1%, ($p$<0.001) and by 22 ± 3%, ($p$=0.01), respectively. In addition, excess amounts of unlabelled $TFPI^{BHK}$ inhibited the endocytosis of $^{125}$I-asialofetuin by 90 ± 6% ($p$<0.001) (Figure 6B).

*Accumulation in kidneys*

The observation that i.v. administered $TFPI^{BHK}$ accumulated in the kidneys encouraged us to investigate the uptake of $TFPI^{BHK}$ *in vitro* on cultures of kidneys cells. To this end, we used a kidney proximal tubule cell line from opossum (OK cells). Here we found that excess amounts of unlabelled RAP had a significant inhibition on both binding and internalization of $^{125}$I- $TFPI^{BHK}$ in OK cells (Table 3).

## DISCUSSION

The present study was carried out to determine the early clearance kinetics, and organ, cell(s) and receptor(s) responsible for the clearance of full length TFPI purified from BHK cells ($TFPI^{BHK}$). We found that $TFPI^{BHK}$ followed biphasic pattern of elimination, similar to the kinetics of TFPI of bacterial origin ($TFPI^{E.Coli}$). However, the clearance during the α-phase was significantly slower for $TFPI^{BHK}$ as compared to $TFPI^{E.Coli}$. Distribution of radiolabeled-ligand after i.v. administration revealed a rapid accumulation of radioactivity in the parenchymal cells (PCs) in the liver, with subsequent accumulation of radioactivity in the gastrointestinal tract over time, indicating that PCs are the principal site for uptake of both forms of TFPI. When $^{125}$I- $TFPI^{BHK}$ was administered along with excess amounts of unlabelled $TFPI^{BHK}$ i.v. or to cultured PCs, delayed blood clearance or reduced uptake in cultured cells were observed, suggesting a receptor-mediated mechanism of uptake. Studies *in vivo* to identify candidate receptors for uptake of $TFPI^{BHK}$ revealed that ASOR, a potent inhibitor of the ASGP-R, prolonged the circulatory survival of $^{125}$I- $TFPI^{BHK}$. This finding along with the *in vitro* results showing that several ligands for the ASGP-R markedly inhibited endocytosis of $TFPI^{BHK}$ in PCs, strongly suggested that ASGP-R is responsible for the PC-mediated clearance of recombinant $TFPI^{BHK}$.

Anatomical distribution of radiolabeled-ligands observed 10 min after i.v. injection of $^{125}$I-TFPI revealed that $TFPI^{E.Coli}$ was cleared mainly by the liver, whereas $TFPI^{BHK}$ was found both in liver and kidneys (Figure 2). Analyses of hepatocellular distribution of radioactivity after injection of radiolabeled $TFPI^{BHK}$ and $TFPI^{E.Coli}$ demonstrated that PC was the principal cellular site of uptake in the liver (Table 1), supporting previous *in vitro* findings that hepatoma-derived cell lines (e.g. HepG2 and $MH_1C_1$ cells) take up $TFPI^{E.Coli}$ via receptor-mediated endocytosis [10]. Previously, SDS-PAGE monitoring of plasma showed that radiolabeled $TFPI^{E.Coli}$ was not proteolyzed for at least 10 min after its i.v. administration [8,

14]. Similarly, we observed only trace amounts of degraded material in blood starting to appear about 20 min after the administration of $TFPI^{E.Coli}$ (Figure 1). In our study, subsequent distribution of recovered radioactivity in various organs collected over time showed a rapid decrease in the radioactivity in the liver, with a concomitant increase in the gastrointestinal tract (Figure 2). These observations suggest that exogenously administered TFPI is preferably taken up by the PCs in the liver, and further transported into the bile, either as intact protein or as degradation products, for subsequent removal via the intestine [31].

Previous studies reporting that pre-administration of RAP prolonged the beta-phase elimination from the circulation of $TFPI^{E.Coli}$ [9], and that cellular degradation of $TFPI^{E.Coli}$ in hepatoma cell-lines were significantly inhibited by RAP [10], suggest that receptor-mediated endocytosis via LRP-1 is the predominant mechanism for uptake and degradation of $TFPI^{E.Coli}$. Since hepatoma-derived cell lines differ from primary cell cultures with regard to receptor expression and endocytic capacity [32, 33], we investigated uptake and degradation of $TFPI^{E.Coli}$ and $TFPI^{BHK}$ in primary cultures of freshly isolated PCs. We found that PCs bind and degrade both forms of TFPI, and that the endocytosis of $TFPI^{BHK}$ is receptor-mediated. Binding of $TFPI^{BHK}$ to PCs reached equilibrium after 2 h of incubation, similar with the kinetics previously observed in HUVECs and Ea.hy926 cells [34].

Further investigations in our study focused on clearance and uptake mechanism of $TFPI^{BHK}$. Interestingly, cross-competitive binding studies *in vitro* with radiolabeled $TFPI^{BHK}$ and $TFPI^{E.Coli}$ and excess amounts of unlabeled $TFPI^{E\text{-}Coli}$ and $TFPI^{BHK}$, respectively, caused no reciprocal inhibition of cellular binding and endocytosis. In agreement with a previous study of recombinant full-length TFPI expressed in mouse C127 cells [13], no effect of RAP was observed in blood clearance *in vivo*, or on cell binding and degradation of $TFPI^{BHK}$ in primary cultures of PCs *in vitro*. These findings strongly suggested that $TFPI^{E.Coli}$ and $TFPI^{BHK}$ do not

share the same receptor for endocytosis, and that LRP-1 is not responsible for the endocytosis of $TFPI^{BHK}$.

The role of the kidneys in binding and degradation of TFPI is unclear. In agreement with previous studies [14], we found only trace amounts of radioactivity retained in the kidneys after i.v. administration of $^{125}$I- $TFPI^{E.Coli}$, whereas substantial amounts of radioactivity was associated with the kidneys after administration of $^{125}$I- $TFPI^{BHK}$ (Figure 2). Our finding is in accordance with a previous study in rabbits, where whole body autoradiography was used to demonstrate distribution of radiolabelled rTFPI (purified from either mouse C127 fibroblasts or human SK hepatoma cells) in both liver and kidneys after i.v. administration [14]. A recent study has shown that only trace amounts of endogenous TFPI accumulates in the urine as native, non-degraded TFPI form in humans, indicating renal leakage rather than active excretion of TFPI into the urine [35]. Since the present study also showed trace amounts of $^{125}$I-$TFPI^{BHK}$ accumulated in the urine over time, the reason behind detection of 25% of radioactivity in the kidneys was further investigated. Fluorescence microscpopy of kidney sections following *in vivo* administration of FITC-$TFPI^{BHK}$, where the FITC adduct is trapped in the lysosomes of cells after endocytosis [36, 37], showed accumulation of the probe in the outer cortex, mainly in cells of the proximal convoluted tubules and to less extent in glomeruli (Figure 3). To date, no studies have investigated the potential reabsorption of TFPI in the kidneys. We present data supporting that the probable mechanism for detection of $TFPI^{BHK}$ in the kidney is by renal reabsorption in the proximal tubules. Opossum kidney (OK) cell is an established cell line resembling the proximal tubule epithelium which expresses megalin and cubilin, two members of the LDL receptor family [27, 28]. Using this cell line, we found that RAP significantly inhibited both binding and internalization of $^{125}$I- $TFPI^{BHK}$. Despite a wide range of ligands shared by both LRP-1 and megalin, there are also ligands that are only recognized by either one of the receptors [38]. The fact that RAP inhibited the $^{125}$I- $TFPI^{BHK}$

uptake in the OK cells but not in the PCs suggests that $TFPI^{BHK}$ may bind to megalin and/or cubilin in the proximal tubule cells via other specific binding sites not found on LRP-1 in the liver PCs. In addition, cellular degradation with subsequent reabsorption of degraded $TFPI^{BHK}$ into the circulation by cells in the proximal tubules could also occur to some extent due to the modest increase in degraded $TFPI^{BHK}$, but not $TFPI^{E.Coli}$ in the circulation, as observed in our study.

Immediate binding to negatively charged heparan-sulfate proteoglycans (HSPGs) at the endothelial surface, most probably due to electrostatic interactions with the positively charged C-terminus of TFPI [8, 11, 39], has been suggested to be responsible for the rapid clearance of $TFPI^{E.Coli}$ from the circulation [9]. HSPGs have been shown to serve either as co-receptors of LRP-1 providing the initial binding of $TFPI^{E.Coli}$ to the cell surface and its subsequent presentation to LRP-1, or function as catabolic receptors themselves, acting independently of LRP-1 [9, 40]. TFPI expressed in mouse fibroblasts ($TFPI^{C127}$) was recently found to be unable to bind to HSPGs at cell surfaces *in vitro* and exhibited a 10-fold increase in plasma half-life when injected in mice compared to $TFPI^{E.Coli}$ *in vivo* [13]. Moreover enzymatic breakdown of glycosaminoglycans (GAGs) chains on HUVEC and Ea·hy926 cells was previously shown not to have an effect on the binding of $TFPI^{BHK}$, and the authors concluded that the binding-site must be different than GAGs [34]. Similarly, we found that neither elimination, nor cellular binding and degradation of $TFPI^{BHK}$ in primary cultures of PCs, were substantially affected by interaction with HSPGs on cell surfaces. The mechanism underlying abrogated interaction of $TFPI^{BHK}$ with the HSPGs at cell surfaces is not known, but may involve intra-molecular quenching of the positively charged basic amino acid residues in the C-terminus by interaction with highly charged anionic sulfate groups at glycosylation sites [13].

Human recombinant $TFPI^{BHK}$ differs from bacterial $TFPI^{E.Coli}$ in molecular weight (42 kDa and 35 kDa, respectively) due to post-translational modifications in mammalian cells involving *N*-linked glycosylation at three potential sites; Asn 117, Asn 167, Asn 228 [4, 5, 41]. The mammalian cells used for synthesis of $TFPI^{BHK}$ in our study, the BHK cells, are known to have a heterogeneous glycosylation pattern. However, under certain culture conditions, changes in the oligosaccharide chains occur and the product secreted by these cells will be partially desialylated [42]. The carbohydrate moiety of plasma glycoproteins is known to play a key role in their plasma clearance [43]. Desialylation and subsequent exposure of the galactose is known to increase the rate of removal of many plasma glycoproteins from the circulation due to recognition by the asialoglycoprotein receptor (ASGP-R). This reduction of intravascular half-life has been found when as little as 25% of the sialic acid has been removed [44]. In addition, glycoproteins containing terminal sugars other than galactose have also been shown to be cleared more rapidly than corresponding sialylated proteins: the affinity of the hepatic ASGP-R is up to 60-fold greater for structures containing *N*-acetyl-galactosamine than for galactose [45]. The fact that our recombinant $TFPI^{BHK}$ is endocytosed specifically by the ASPG-R provides evidence that this type of TFPI carries galactose and/or *N*-acetyl-galactosamine in the end position of its glycan structures.

In conclusion, we have demonstrated that the clearance of recombinant $TFPI^{BHK}$ involves receptor-mediated endocytosis via ASGP-R in PCs, a different mechanism than the clearance of $TFPI^{E.Coli}$. It appears that $TFPI^{BHK}$ most probably is not completely sialylated. The extent of sialylation of TFPI in mammalian cells remains to be investigated and strategies to completely glycosylate the protein would be needed to optimize pharmacokinetic properties and thereby potential therapeutic use.

**Table 1. Hepatocellular distribution of of $^{125}$I-b-TFPI and $^{125}$I-m-TFPI**

At 15 min following i.v. administration of $^{125}$I-b-TFPI (white bars) and $^{125}$I-m-TFPI (gray bars), the liver cells were dispersed by collagenase perfusion and the amount of radioactivity per million cells was measured in suspension of parenchymal cells (PCs) and non parencymal cells (NPCs) [sinusoidal endothelial cells (LSECs) and Kupffer cells (KCs)]. The uptake per cell in the total liver was calculated based on the knowledge that the ratio between KC, LSEC and PC in rat liver is 1:2.5:7.7 [23].

| Ligand | Radioactivity (% of total liver cell population) | | N |
|---|---|---|---|
| | PCs | NPCs | |
| $^{125}$I-b-TFPI | 80.7 ± 11.9 | 19.3 ± 11.9 | 3 |
| $^{125}$I-m-TFPI | 95.7 ± 1.7 | 4.3 ± 1.7 | 6 |

**Table 2**. **Specificity of m-TFPI clearance *in vivo***

$^{125}$I-m-TFPI (0.5 nM) was injected alone or 1 min after administration of 200-fold molar excess of unlabeled mTFPI, 40 mg/kg Protamine, 50 mg/kg RAP or 15 mg/kg ASOR into a lateral tail vein and radioactivity was measured in blood samples over time. Radioactivity in blood 1 min after injection was taken as 100%. The clearance was fitted to two-phase exponential decay. The values are mean ± SEM. **$p$<0.01 compared to control (0.5 nM $^{125}$I-m-TFPI alone).

| Ligands | $t_{1/2}\alpha$ (min) | $t_{1/2}\beta$ (min) | N |
|---|---|---|---|
| 0.5 nM $^{125}$I-m-TFPI | 1.95 ± 0.10 | 25.47 ± 1.47 | 10 |
| +200-fold molar excess m-TFPI | 2.84 ± 0.05** | 40.47 ± 2.00** | 5 |
| +50 mg/kg RAP | 2.00 ± 0.27 | 19.85 ± 0.76 | 6 |
| +15 mg/kg ASOR | 2.96 ± 0.10** | 27.84 ± 0.01 | 3 |
| +40 mg/kg Protamine | 2.03 ± 0.19 | 26.14 ± 1.71 | 4 |

**Table 3**. **Binding of m-TFPI to kidney proximal tubule cells**

Monolayer cultures of OK cells were incubated with 0.5 nM $^{125}$I-m-TFPI in the presence or absence of 500 nM RAP. Cell surface bound and internalized m-TFPI was measured after 1h of incubation at 37°C as described in Materials and Methods. Results are presented as percent of control. 100% corresponds to about 8.51 fmol m-TFPI.

| | $^{125}$I-m-TFPI alone | + RAP | *p* |
|---|---|---|---|
| $^{125}$I-m-TFPI bound to cell surface | 83.69 ± 3.81 | 56.35 ± 7.33 | 0.04 |
| $^{125}$I-m-TFPI internalized | 15.79 ± 2.84 | 5.12 ± 3.94 | 0.02 |

## FIGURE LEGENDS

**Figure 1 Blood clearance of radiolabeled TFPI**

$^{125}$I-TFPI$^{E.Coli}$ and $^{125}$I-TFPI$^{BHK}$ (0.60 μg/kg in 0.5 mL physiological saline) were injected into a lateral tail vein, and blood samples (25μl) were collected in 0.5 ml water after various time points and immediately mixed with 0.75 ml 20% TCA, 0.5% PTA. Radioactivity in blood 0.5 min after injection was taken as 100%. The clearance was fitted to two-phase exponential decay. Open symbols represent acid soluble radioactivity (degraded TFPI). Closed symbols represent acid-precipitable radioactivity (non-degraded TFPI). Inset shows α and β half-lives, describing the kinetics of the initial and terminal clearance phases. The values are mean ± SEM from 10 separate experiments.

**Figure 2 Anatomical distribution of radiolabeled TFPI**

Trace amounts of $^{125}$I-TFPI$^{E.Coli}$ (A) and $^{125}$I-TFPI$^{BHK}$ (B) (0.25 μg/kg in 0.5 mL physiological saline) were injected into a lateral tail vein. At different times after injection the organs were washed free of blood, removed and analyzed for radioactivity. The results are presented as percentage of total recovered radioactivity. Radioactivity of tissues and organs other than those shown in the figure was less than 2%. Bars are mean ± S.D. for four separate experiments.

**Figure 3 Fluorescence micrographs of liver sections (A, B) and kidneys (C, D)**

At 15 min following i.v. administration of 30 μg/kg FITC-TFPI$^{BHK}$ in 0.5 ml physiological saline, liver and kidneys were dissected out, fixed in 4% formaldehyde, prepared and sectioned for fluorescence microscopy. Sections were examined with an Axiophot photomicroscope (Carl Zeiss, Oberkochen, Germany). Photomicrographs were taken with a Nikon DS 5MC digital camera. In liver, the fluorescence was observed in the parenchymal cells (arrows) (A) and in cells lining the sinusoids (arrows) (B). In kidneys, the fluorescence

was observed in the outer cortex (bar) (C), mainly in the cells of the proximal convoluted tubules (arrows) (D).

**Figure 4 Kinetics of endocytosis of $^{125}$I-TFPI$^{E.Coli}$ (A) and $^{125}$I-TFPI$^{BHK}$ (B) in PCs**

$^{125}$I-TFPI$^{E.Coli}$ and $^{125}$I-TFPI$^{BHK}$ (0.5 nM) were incubated with cultures of PCs in 2 cm$^2$ diameter dishes at 37°C, and cell-associated (■) and degraded (□) ligand were determined after various periods of time as described in the Materials and Methods section. Total endocytosis (●) is the sum of cell-associated and degraded ligand. Results are presented in fmol TFPI/$10^6$ PCs. Bars are means ± S.D. for four separate experiments.

**Figure 5 Endocytosis of $^{125}$I-TFPI$^{BHK}$ in cultured PCs**

Monolayer cultures of PCs were incubated with 0.5 nM $^{125}$I-TFPI$^{BHK}$ alone, in PCs pretreated with protamine (100 μg/ml), or excess amounts of unlabelled TFPI$^{BHK}$ (500-fold molar) or RAP (100 μg/ml). Cell-associated (white bars) and degraded (gray bars) ligand were determined after 2 h of incubation at 37°C as described in Materials and Methods. Results are given as percent of Control. 100% corresponds to about 35 fmol TFPI$^{BHK}$. Bars are means ± SEM for four to eight separate experiments.

**Figure 6 Specificity of Endocytosis of $^{125}$I-TFPI$^{BHK}$ in cultured PCs**

(A) Monolayer cultures of PCs were incubated with 0.5 nM $^{125}$I-TFPI$^{BHK}$ in the absence or presence of excess amounts of unlabelled ASOR, asialofetuin, asialo-FVIIa, ovalbumin (100 μg/ml) or Galactose (50 mM) (A). (B) Monolayer cultures of PCs were incubated with trace amounts of $^{125}$I-asialofetuin in the absence or presence of excess amounts of unlabelled TFPI$^{BHK}$ (100 μg/ml). Cell-associated (white bars) and degraded (gray bars) ligand were determined after 2 h of incubation at 37°C. Results are given as percent of Control. 100% corresponds to about 35 fmol TFPI$^{BHK}$. Bars are means ± SD for 3 separate experiments.

**Figure 1**

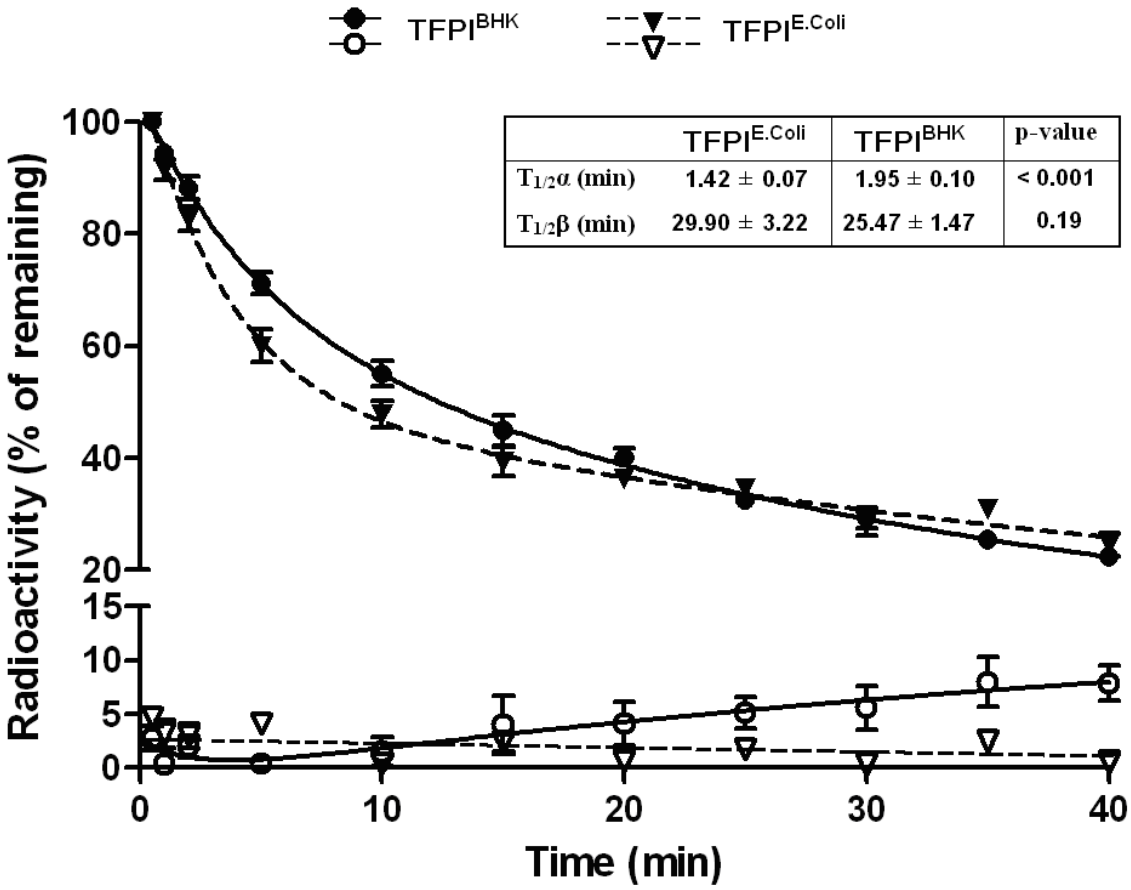


| | $TFPI^{E.Coli}$ | $TFPI^{BHK}$ | p-value |
|---|---|---|---|
| $T_{1/2}\alpha$ (min) | 1.42 ± 0.07 | 1.95 ± 0.10 | < 0.001 |
| $T_{1/2}\beta$ (min) | 29.90 ± 3.22 | 25.47 ± 1.47 | 0.19 |

**Figure 2**

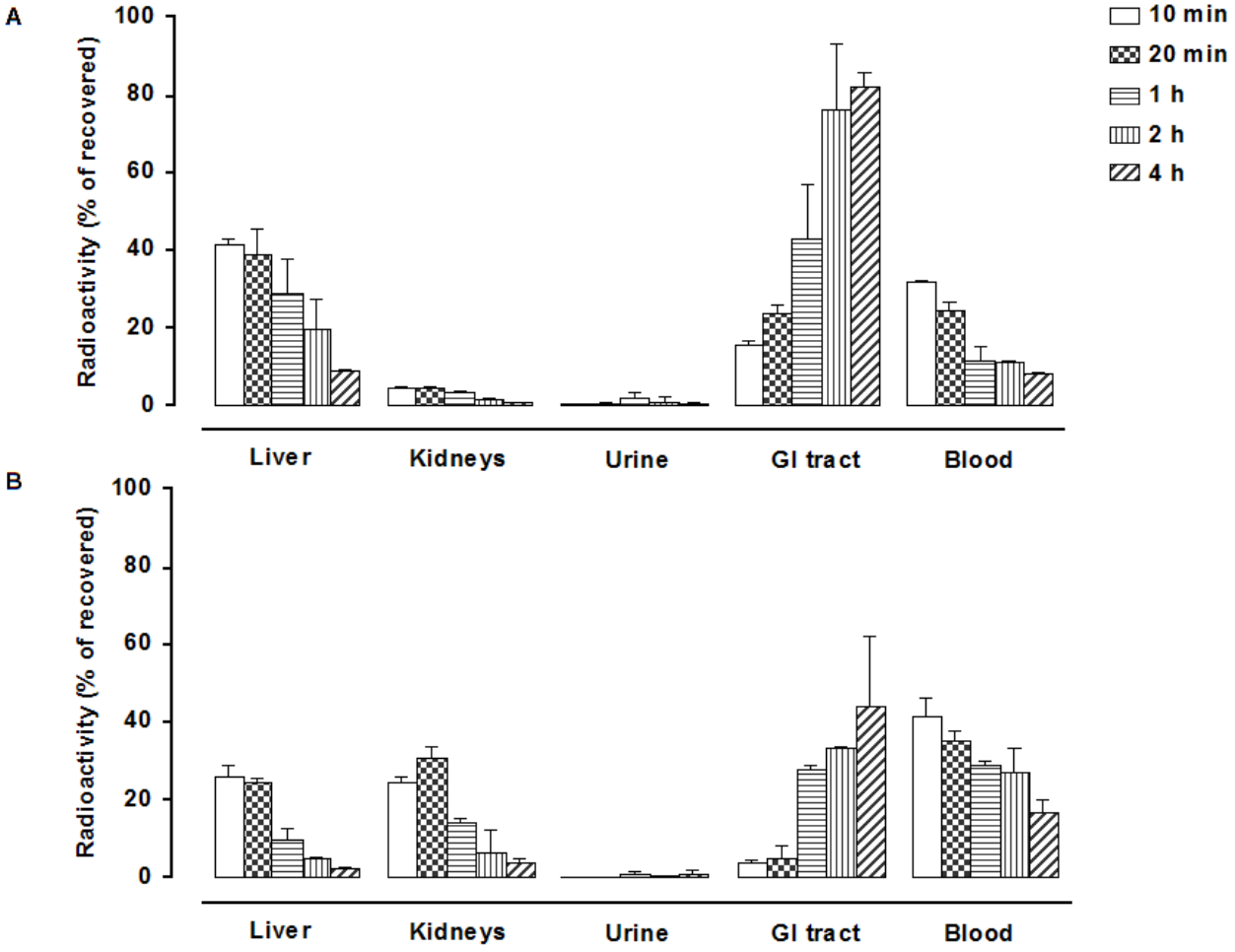
A
B
Radioactivity (% of recovered)
100
80
60
40
20
0
Liver
Kidneys
Urine
GI tract
Blood
10 min
20 min
1 h
2 h
4 h

**Figure 3**

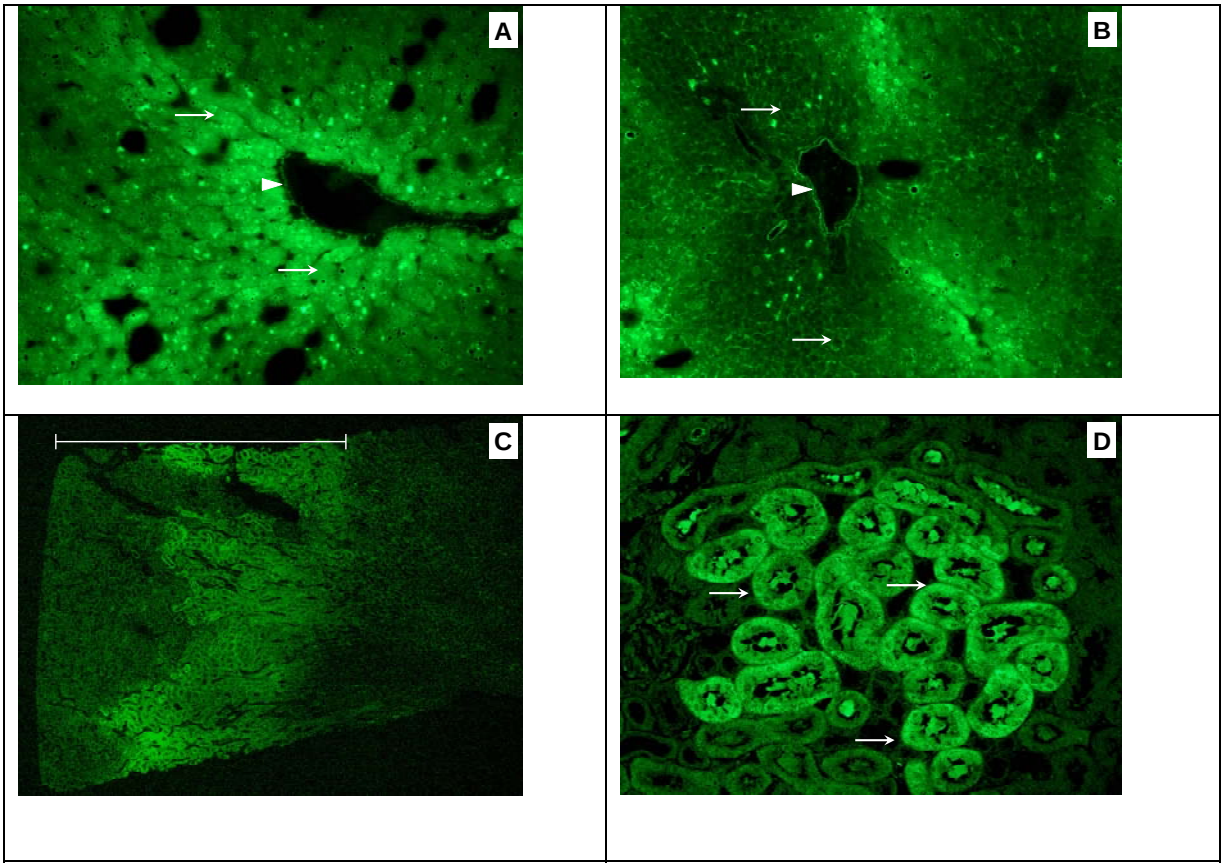

**Figure 4**

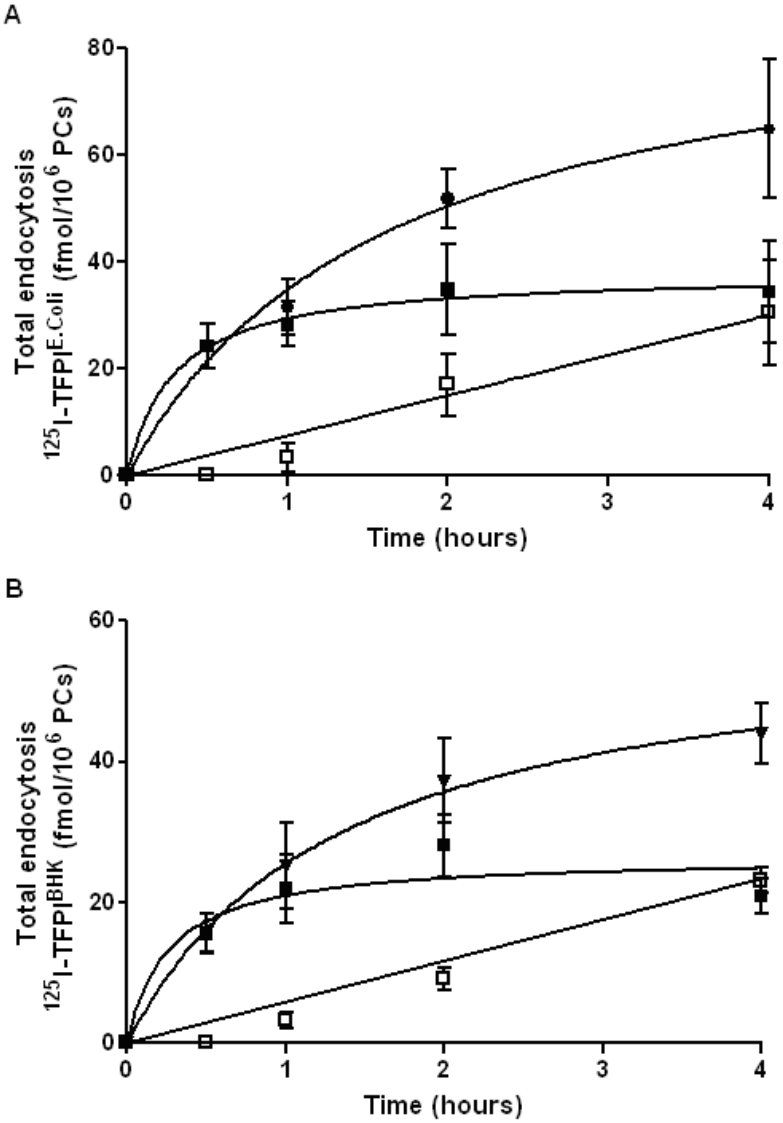
A
Total endocytosis
$^{125}$I-TFPI$^{E.Coli}$ (fmol/10$^6$ PCs)
80
60
40
20
0
0
1
2
3
4
Time (hours)
B
Total endocytosis
$^{125}$I-TFPI$^{BHK}$ (fmol/10$^6$ PCs)
60
40
20
0
0
1
2
3
4
Time (hours)

**Figure 5**

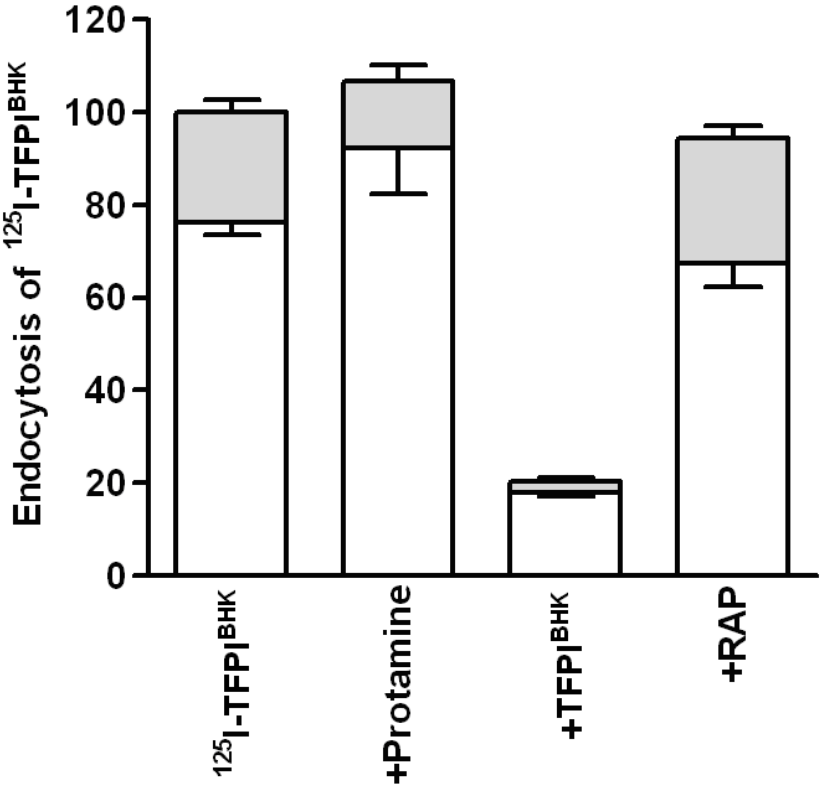
Endocytosis of 125I-TFPIBHK
120
100
80
60
40
20
0
125I-TFPIBHK
+Protamine
+TFPIBHK
+RAP

**Figure 6**

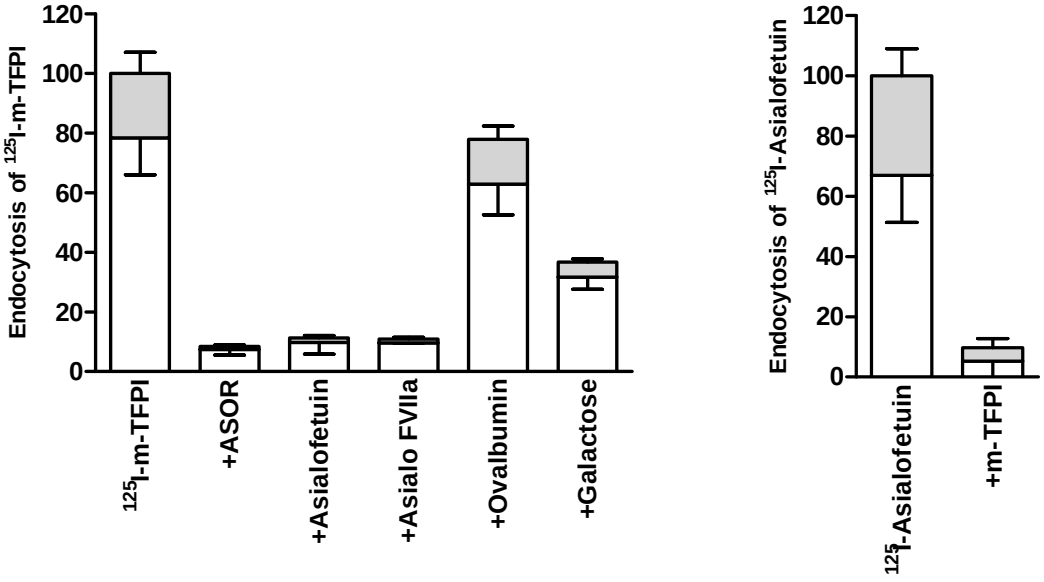
Endocytosis of 125I-m-TFPI
120
100
80
60
40
20
0
125I-m-TFPI
+ASOR
+Asialofetuin
+Asialo FVIIa
+Ovalbumin
+Galactose
Endocytosis of 125I-Asialofetuin
120
100
80
60
40
20
0
125I-Asialofetuin
+m-TFPI

## REFERENCES


1. **Rapaport, S.I. and L.V. Rao, *The tissue factor pathway: how it has become a "prima ballerina"*. Thromb Haemost, 1995. 74(1): p. 7-17.**
2. **Broze, G.J., Jr. and J.P. Miletich, *Characterization of the inhibition of tissue factor in serum.* Blood, 1987. 69(1): p. 150-5.**
3. **Rao, L.V. and S.I. Rapaport, *Studies of a mechanism inhibiting the initiation of the extrinsic pathway of coagulation.* Blood, 1987. 69(2): p. 645-51.**
4. **Wun, T.C., et al., *Cloning and characterization of a cDNA coding for the lipoprotein-associated coagulation inhibitor shows that it consists of three tandem Kunitz-type inhibitory domains.* J Biol Chem, 1988. 263(13): p. 6001-4.**
5. **Broze, G.J., Jr., et al., *Heterogeneity of plasma tissue factor pathway inhibitor.* Blood Coagul Fibrinolysis, 1994. 5(4): p. 551-9.**
6. **Crawley, J.T. and D.A. Lane, *The haemostatic role of tissue factor pathway inhibitor.* Arterioscler Thromb Vasc Biol, 2008. 28(2): p. 233-42.**
7. **DelGiudice, L.A. and G.A. White, *The role of tissue factor and tissue factor pathway inhibitor in health and disease states.* J Vet Emerg Crit Care (San Antonio), 2009. 19(1): p. 23-9.**
8. **Warshawsky, I., et al., *The carboxy terminus of tissue factor pathway inhibitor is required for interacting with hepatoma cells in vitro and in vivo.* J Clin Invest, 1995. 95(4): p. 1773-81.**
9. **Narita, M., et al., *Two receptor systems are involved in the plasma clearance of tissue factor pathway inhibitor in vivo.* J Biol Chem, 1995. 270(42): p. 24800-4.**
10. **Warshawsky, I., G.J. Broze, Jr., and A.L. Schwartz, *The low density lipoprotein receptor-related protein mediates the cellular degradation of tissue factor pathway inhibitor.* Proc Natl Acad Sci U S A, 1994. 91(14): p. 6664-8.**
11. **Ho, G., G.J. Broze, Jr., and A.L. Schwartz, *Role of heparan sulfate proteoglycans in the uptake and degradation of tissue factor pathway inhibitor-coagulation factor Xa complexes.* J Biol Chem, 1997. 272(27): p. 16838-44.**
12. **Wurm, F.M., *Production of recombinant protein therapeutics in cultivated mammalian cells.* Nat Biotechnol, 2004. 22(11): p. 1393-8.**
13. **Ho, G., et al., *Recombinant full-length tissue factor pathway inhibitor fails to bind to the cell surface: implications for catabolism in vitro and in vivo.* Blood, 2000. 95(6): p. 1973-8.**
14. **Palmier, M.O., et al., *Clearance of recombinant tissue factor pathway inhibitor (TFPI) in rabbits.* Thromb Haemost, 1992. 68(1): p. 33-6.**
15. **Pedersen, A.H., et al., *Recombinant human extrinsic pathway inhibitor. Production, isolation, and characterization of its inhibitory activity on tissue factor-initiated coagulation reactions.* J Biol Chem, 1990. 265(28): p. 16786-93.**
16. **Bregengaard, C., et al., *Pharmacokinetics of full length and two-domain tissue factor pathway inhibitor in combination with heparin in rabbits.* Thromb Haemost, 1993. 70(3): p. 454-7.**
17. **Eap, C.B. and P. Baumann, *Isoelectric focusing of alpha-1 acid glycoprotein (orosomucoid) in immobilized pH-gradients with 8M urea: detection of its desialylated variants using an alkaline phosphatase-linked secondary antibody system.* Electrophoresis, 1988. 9(10): p. 650-4.**
18. **Mego, J.L., F. Bertini, and J.D. McQueen, *The use of formaldehyde-treated 131-I-albumin in the study of digestive vacuoles and some properties of these particles from mouse liver.* J Cell Biol, 1967. 32(3): p. 699-707.**

19. **Markwell, M.A., *A new solid-state reagent to iodinate proteins. I. Conditions for the efficient labeling of antiserum.* Anal Biochem, 1982. 125(2): p. 427-32.**
20. **Hellevik, T., A. Bondevik, and B. Smedsrod, *Intracellular fate of endocytosed collagen in rat liver endothelial cells.* Exp Cell Res, 1996. 223(1): p. 39-49.**
21. **Smedsrod, B. and M. Einarsson, *Clearance of tissue plasminogen activator by mannose and galactose receptors in the liver.* Thromb-Haemost, 1990. 63(1): p. 60-6.**
22. **Waynforth, H.B. and P.A. Flecknell, *Experimental and Surgical Technique in the Rat.* San Diego, CA; Academic; , 1992(Second Edition): p. 342.**
23. **Pertoft, H. and B. Smedsrod, *Separation and characterization of liver cells.* In: Pretlow TG, Pretlow TPNY, eds. Cell Separation Methods and Selected Applications. Volume 4. Academic Press, 1987: p. 1-24.**
24. **Smedsrod, B., et al., *Circulating C-terminal propeptide of type I procollagen is cleared mainly via the mannose receptor in liver endothelial cells.* Biochem J, 1990. 271(2): p. 345-50.**
25. **Van Berkel, T.J., et al., *Uptake and catabolism of modified LDL in scavenger-receptor class A type I/II knock-out mice.* Biochem J, 1998. 331 ( Pt 1): p. 29-35.**
26. **Smedsrod, B. and H. Pertoft, *Preparation of pure hepatocytes and reticuloendothelial cells in high yield from a single rat liver by means of Percoll centrifugation and selective adherence.* J Leukoc Biol, 1985. 38(2): p. 213-30.**
27. **Zhai, X.Y., et al., *Cubilin- and megalin-mediated uptake of albumin in cultured proximal tubule cells of opossum kidney.* Kidney Int, 2000. 58(4): p. 1523-33.**
28. **Hammad, S.M., et al., *Megalin acts in concert with cubilin to mediate endocytosis of high density lipoproteins.* J Biol Chem, 2000. 275(16): p. 12003-8.**
29. **Berg, T., et al., *Intracellular transport of asialoglycoproteins in rat hepatocytes. Evidence for two subpopulations of lysosomes.* Exp Cell Res, 1985. 161(2): p. 285-96.**
30. **Weigel, P.H. and J.H. Yik, *Glycans as endocytosis signals: the cases of the asialoglycoprotein and hyaluronan/chondroitin sulfate receptors.* Biochim Biophys Acta, 2002. 1572(2-3): p. 341-63.**
31. **Ghibellini, G., E.M. Leslie, and K.L. Brouwer, *Methods to evaluate biliary excretion of drugs in humans: an updated review.* Mol Pharm, 2006. 3(3): p. 198-211.**
32. **Hjortoe, G., et al., *Factor VIIa binding and internalization in hepatocytes.* J Thromb Haemost, 2005. 3(10): p. 2264-73.**
33. **Planas-Bohne, F., W. Jung, and M. Neu-Muller, *Uptake of 59Fe and 239Pu by rat liver cells and human hepatoma cells.* Int J Radiat Biol Relat Stud Phys Chem Med, 1985. 48(5): p. 797-805.**
34. **Iversen, N., et al., *Binding of tissue factor pathway inhibitor to cultured endothelial cells-influence of glycosaminoglycans.* Thromb Res, 1996. 84(4): p. 267-78.**
35. **Brodin, E., et al., *Intravascular release and urinary excretion of tissue factor pathway inhibitor during heparin treatment.* J Lab Clin Med, 2004. 144(5): p. 246-53; discussion 226-7.**
36. **Oie, C.I., et al., *Liver sinusoidal endothelial cells are the principal site for elimination of unfractionated heparin from the circulation.* Am J Physiol Gastrointest Liver Physiol, 2008. 294(2): p. G520-8.**
37. **Hellevik, T., et al., *Transport of residual endocytosed products into terminal lysosomes occurs slowly in rat liver endothelial cells.* Hepatology, 1998. 28(5): p. 1378-89.**

**38.** **May, P. and J. Herz*, LDL receptor-related proteins in neurodevelopment.* Traffic, 2003. 4(5): p. 291-301.**
**39.** **Sandset, P.M., U. Abildgaard, and M.L. Larsen, *Heparin induces release of extrinsic coagulation pathway inhibitor (EPI).* Thromb Res, 1988. 50(6): p. 803-13.**
**40.** **Warshawsky, I., et al., *The low density lipoprotein receptor-related protein can function independently from heparan sulfate proteoglycans in tissue factor pathway inhibitor endocytosis.* J Biol Chem, 1996. 271(42): p. 25873-9.**
**41.** **Novotny, W.F., et al., *Purification and characterization of the lipoprotein-associated coagulation inhibitor from human plasma.* J Biol Chem, 1989. 264(31): p. 18832-7.**
**42.** **Grabenhorst, E., et al., *Genetic engineering of recombinant glycoproteins and the glycosylation pathway in mammalian host cells.* Glycoconj J, 1999. 16(2): p. 81-97.**
**43.** **Ashwell, G. and J. Harford, *Carbohydrate-specific receptors of the liver.* Annu Rev Biochem, 1982. 51: p. 531-54.**
**44.** **Van Den Hamer, C.J., et al., *Physical and chemical studies on ceruloplasmin. IX. The role of galactosyl residues in the clearance of ceruloplasmin from the circulation.* J Biol Chem, 1970. 245(17): p. 4397-402.**
**45.** **Kolatkar, A.R., et al., *Mechanism of N-acetylgalactosamine binding to a C-type animal lectin carbohydrate-recognition domain.* J Biol Chem, 1998. 273(31): p. 19502-8.**